

Analysis of Ribbed Dome Structures Using Finite Element Method

Ankit Jena¹, Rojanil Senapati²

¹Assistant Professor, Department of Civil Engineering, Gandhi Institute For Technology (GIFT), Bhubaneswar

²Assistant Professor, Department of Civil Engineering, Gandhi Engineering College, Bhubaneswar

Abstract: This paper deals with the linear finite element analysis of ribbed domes. Stresses and deformations of ribbed dome were analysed. The finite element model of these domes were prepared and analysed by using STAAD Pro V8i software. Plate element is used to simulate the bricks which fill the areas between ribs and rings. Beam element is used to simulate the standard steel sections of ribs and rings. A dome similar to that of Imam Mohammed Baqir Alsadir shrine's, in North of Najaf – Iraq constructed in 2012, is considered as a case study. The main structural members of the dome consist of steel I – section used as ribs and double channel steel – section used for rings. The panels between ribs and rings are filled with bricks of 240 mm thick. Loads are applied as uniformly distributed per unit area of shell surface. Many parameters are considered as variables in the dome analysis including the spacing between ribs, the spacing between rings and the conditions of connection between brick and steel members (release of moment and forces at nodes between brick and steel). Brick dome with constant thickness of 240 mm is also analysed to make a comparison with ribbed domes. The results show that the conditions of connection between brick and steel members have considerable effect on obtained stresses and displacements. Tensilemeridional stresses are obtained in brick of ribbed domes when the spacing between ribs is increased. The maximum horizontal displacements are obtained at point with embrace angle $\phi = 90^\circ$.

Keywords: Ribbed Domes, Brick Domes, Steel Ribs, Steel Rings, Finite Element Analysis

I. Introduction

Domes are one of the oldest and well established structural forms and have been used in construction since the earliest times. They are of special interest to engineers as they enclose a maximum space with minimum surface and are very economical in terms of consumption of constructional materials. The ribbed dome is the earliest type of braced dome that has been constructed. A ribbed dome consists of a number of identical meridional girders or trusses, interconnected at the crown by compression ring [1]. Domes are thin shells in the form of surfaces of revolution having a thickness t , of $R/t > 20$ where R is the minimum radius of curvature [2]. This thickness of the shell may vary across its surface, e.g. it may be increased, if possible, in some areas to prevent cracking.

Chacko et. al [3], studied ribbed spherical dome with rigid joints. The proposed dome was modelled and analysed by using software's ANSYS and Staad.Pro for different rise to span ratios and different load cases. The results showed that the failure of ribbed dome structure is due to buckling of structure. It is recommended to choose rise to span ratio in between 0.3 -0.35 for ribbed domes which can improve the performance of dome. Kaveha et. al [4], developed an optimum topology design algorithm based on the Hybrid Big Bang – Big Crunch optimization (HBB-BC) method for the schwedler and ribbed domes. In this study, the obtained results showed that increasing the number of rings does not improve the performance of the dome. Al-Zaidi [5] conducted an analysis on reinforced concrete (R.C.) ribbed domes. The research dealt with the linear F.E. analysis of large diameter R.C. ribbed domes resting at the base on ring R.C. rectangular beam and then on R.C. columns that are equally spaced along the periphery of a dome base. The analysis was carried out using the computer program SAP 2000 version 14. Many parameters were considered as variables including shell thickness, depth of rib, ring beam size, length of columns, rise of dome, diameter of dome, excluding ribs, adding ring beam at crown, the case of no columns and the case of additional uniform load on dome. It was found that increasing the depth of ribs from (0.4 m to 1 m) causes the internal stresses in the shell to decrease by 17% for maximum tensile stress and 3% for maximum compressive stress (both occurring near the ring beam location). Also increasing the size of the ring beam from (0.5×0.5 m to 1×1 m) led the internal stresses in the shell to decrease by 20% for maximum compressive stress and 72% for maximum tensile stress.

Lau [6] carried out a case of study on Farag Ibn Barquq, Cairo, Egypt brick and stone masonry dome. The geometric parameters were median radius of curvature of 8.2 m, rise from springing of 9.8 m, span at base of 14.3 m, thickness of 0.36 m, and the angle of embrace (\square) in the range of zero to 83 degree. The stability of the dome was investigated by using three different methods; traditional thrust line analysis, the membrane theory, and the modified thrust line analysis. The dome was analyzed as a lune with $\square = 15^\circ$ under uniform

axisymmetric loads. It was concluded that the traditional thrust line analysis and the membrane theory failed to clarify the stability of the dome.

In this paper, a dome is analysed as a brick dome with constant thickness of 240 mm and as a ribbed dome having steel ribs and rings and brick filling the areas between them. Rigid joints are assumed between steel members. Six cases are modeled to represent the ribbed dome. The numbers of ribs are 12, 16, and 24 equally spaced along the circumference of dome, at plan angle of (15, 22.5, and 30 Degrees) respectively. Rings are provided each 1.5 m and 3 m across the height of the dome.

II. Geometry Ofshell

In this paper specific dome is studied with base diameter (D) of 23.6 m and height (H) of 18 m as shown in Fig. (1).

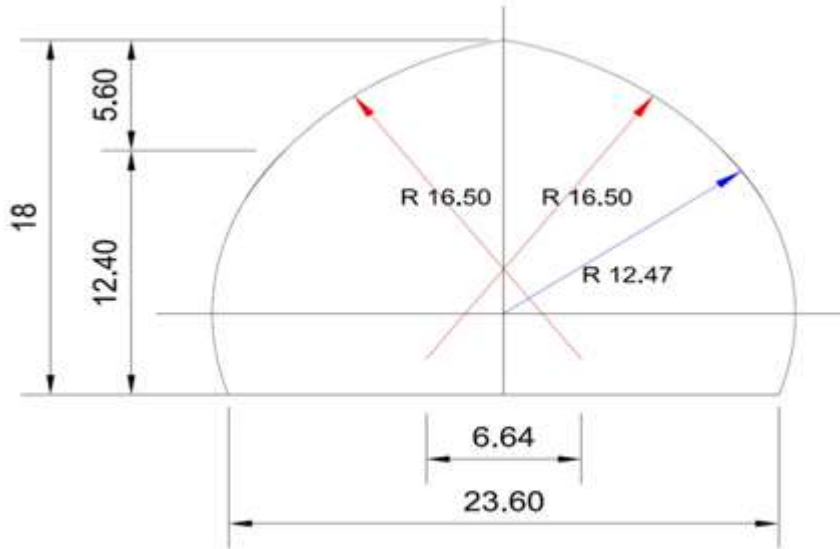


Figure (1) Geometry of used Dome

This geometry is similar to the dome of Imam Mohammed Baqir Alsadir shrine's in North of Najaf – Iraq constructed in 2012. The main structural members of the dome consist of steel I – section UB 356 × 171 × 51 kg/m used as ribs and steel double channel – section CH 260 × 90 × 35 kg/m used for rings. The areas between ribs and rings are filled with bricks of 240 mm thick. The dome rests on reinforced concrete rectangular beam of 400 mm width and 900 mm high. The details of analysed models are shown in Table (1). The same steel sections are used in all models. These sections are the largest obtained sections from the design of all analysed models. The same dome is analysed as a brick dome of 240 mm thickness and without ribs and rings resting on R.C. rectangular beam of 400 mm width and 900 mm high to restrain the dome movement due to thrust force.

Table (1) Details of ribbed dome models

| Model No. | Plan angle (Degree) | Spacing between rings (meter) | Size of rib (mm x mm x kg/m) | Size of ring (mm x mm x kg/m) |
|-----------|---------------------|-------------------------------|------------------------------|-------------------------------|
| RD1 | 15 | 1.5 | UB 356 × 171 × 51 | D - CH 260 × 90 × 35 |
| RD2 | 15 | 3 | UB 356 × 171 × 51 | D - CH 260 × 90 × 35 |
| RD3 | 22.5 | 1.5 | UB 356 × 171 × 51 | D - CH 260 × 90 × 35 |
| RD4 | 22.5 | 3 | UB 356 × 171 × 51 | D - CH 260 × 90 × 35 |
| RD5 | 30 | 1.5 | UB 356 × 171 × 51 | D - CH 260 × 90 × 35 |
| RD6 | 30 | 3 | UB 356 × 171 × 51 | D - CH 260 × 90 × 35 |

III. Materials Properties Ofdome:

The brick material is assumed as equivalent single material [7]. The properties of this material are shown in Table (2). The steel sections have a modulus of elasticity $E = 2 \times 10^5$ MPa, and yield strength $f_y = 275$ MPa

Table (2) Brick properties [7]

| Modulus of Elasticity (E_m)MPa | Modulus of rigidity (G)MPa | Poisson's Ratio (ν) | Density (γ) (kN/m ³) | compressive strength (f'_m)MPa | Allowable compressive stress (f_c) MPa | Allowable tensile stress (f_t) MPa |
|------------------------------------|----------------------------|---------------------------|---|------------------------------------|--|--|
| 9000 | 3600 | 0.15 | 18 | 13 | 0.80 | 0.20 |

IV. Finite Element Analysis:

The finite element method is a powerful technique to solve the complex problems in structural engineering. The finite element models for the considered domes were prepared and analysed by using STAAD Pro V8i software. Plate element of six degrees of freedom at each node was used to simulate the bricks which fill the areas between ribs and rings. Beam element of six degrees of freedom at each node was used to simulate the standard steel sections of ribs and rings. The total number of plate element used in the dome model was 5376 element, and the total number of ribs and rings elements was 2496. This number of elements is decided after examining different number of elements to calculate the maximum displacement of the structure. Loads are applied as uniformly distributed on surface area of the dome. Dead load of 1 kN for finishing materials in addition to self-weight and 1 kN roof live load are applied in global Y-direction. Many parameters are considered as variables in the dome analysis including the spacing between ribs (plan angle \square equal to 15° , 22.5° , and 30°), the spacing between rings (1.5 and 3 m) and the conditions of connection between bricks and steel members (release of moment and forces at nodes between brick and steel). In the simulation of condition of connection between the bricks and steel sections releasing of M_x , M_y , M_z and F_y at the top rings and of M_x , M_y , M_z , F_y and F_x for bottom rings and vertical direction along the ribs are used as shown in Fig (2). Stresses and deflections of the dome are considered as the criteria of failure in bricks. Ribbed domes with different distributions of steel ribs and rings are used to find the suitable angle of rib distribution and spacing betweenrings.

Also a brick dome of constant thickness 240 mm and without ribs and rings is analysed to make a comparison between masonry and ribbed domes. R.C. rectangular beam of 400 mm width and 900 mm high is used to support the dome as fixed ends boundaryconditions.

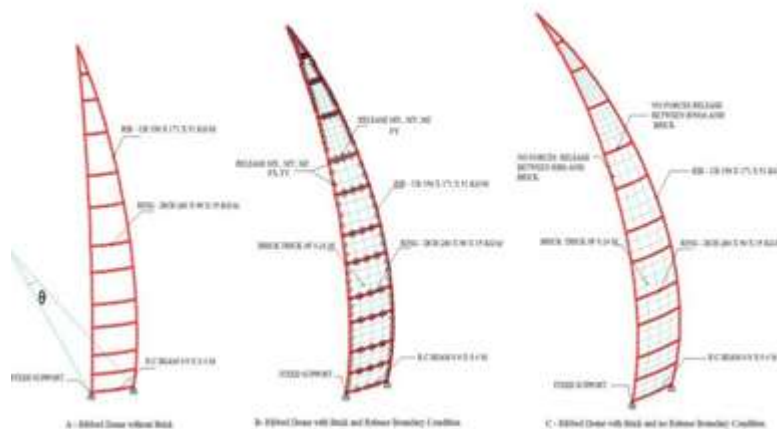


Figure (2) Details of finite element models

V. Results:

The finite element analysis is conducted for ribbed domes having different spacing between ribs and rings. Six models of ribbed domes are prepared and analysed using Staadpro V8i. Each model is analysed three times with different treatment of interaction between ribs and rings and the brick. First, each model is analysed by considering the brick as a load acting on the ribs and rings, this analysis is referred to as Trt-1. Then the model is analysed with discretization of brick into elements, as the ribs and rings, and using the facility of releasing given by the software. This is done by releasing of M_x , M_y , M_z and F_y at the top rings and of M_x , M_y , M_z , F_y and F_x for bottom rings and for vertical direction along the ribs, this analysis is referred to Trt-2. In the third treatment the dome is discretised as in the second one, but no release in boundary condition is used, Trt-3. The results of ribbed dome are compared with brick dome to investigate the effect of steel ribs and rings on the stresses and deflection.

1.1 Stresses:

The stresses in steel sections of all cases are less than the yield stress of steel sections as shown in Fig (3). Also, stresses in ribs increase when plan angle (\square) increases. Models analysed by using treatment method Trt-2 give values of stresses less than those of Trt-1 method. This may be because of existing brick works as a bracing for steel sections.

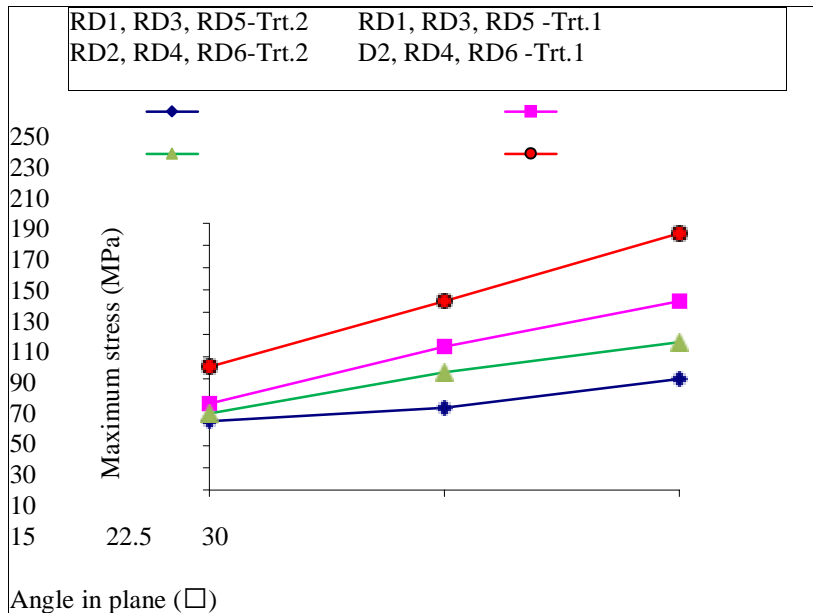


Figure (3) Maximum stresses in steel ribs

The hoop compression stresses of brick are illustrated in Fig (4). It is clear from the figure that all models give a stress which is smaller than the allowable compressive stress of brick (0.8 MPa). Model RD5 with Trt-2 analysis has a larger value of compressive stress as compared with the others models. This model has larger spacing between ribs. Furthermore, crushing does not occur in all models because of the applied compressive stresses are smaller than allowable compressive strength of brick. The figure also shows that when using Trt-3 method of analysis, the maximum stress remain constant for different plan angle (\square). This reveals that the effect of ribs and rings becomes ineffectual if this treatment of interaction between bricks and steel ribs and rings is used.

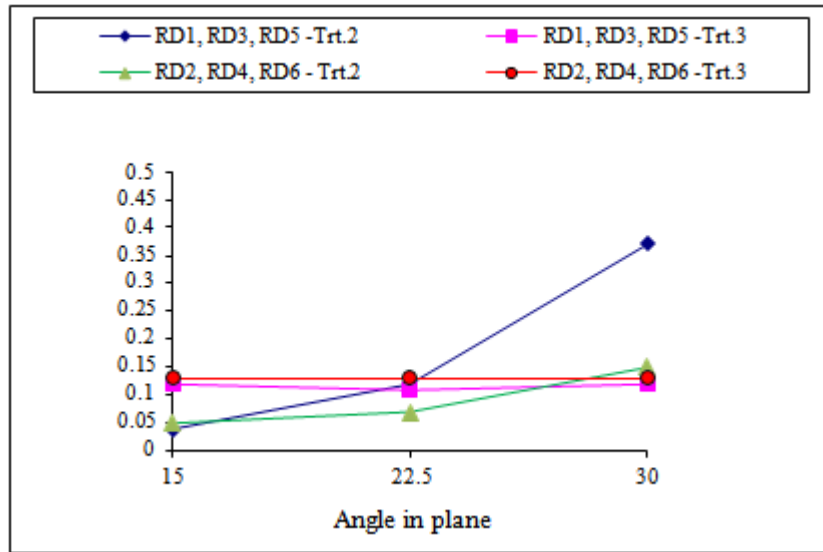


Figure (4) Maximum hoop compression stress in brick

For the hoop tension stresses, Fig. (5) reveals the effect of plan angle and spacing between rings on these stresses in ribbed domes. When the plan angle increases from 15° to 22.5°, models RD1, RD2, RD3 and RD4 with Trt-2 analysis show increase in the tensile stresses, but these stresses are still less than the permissible limit (0.2 MPa). When the plan angle is 30°, Trt-2 analysis gives tensile stresses in brick for RD5 and RD6 of approximately 0.35 MPa which is more than the allowable tensile stress of brick. Different behaviour is obtained in analysis Trt-3, the tensile stresses are much greater than the allowable tensile stress of brick, and this is similar to brick dome as shown in table (3). These results reveal that in analysis Trt-3 the effect of ribs becomes insignificant and the ribbed dome behaves like one without ribs. However, the spacing of steel rings seems to have little effect on tensile stresses in Trt-3 method of analysis.

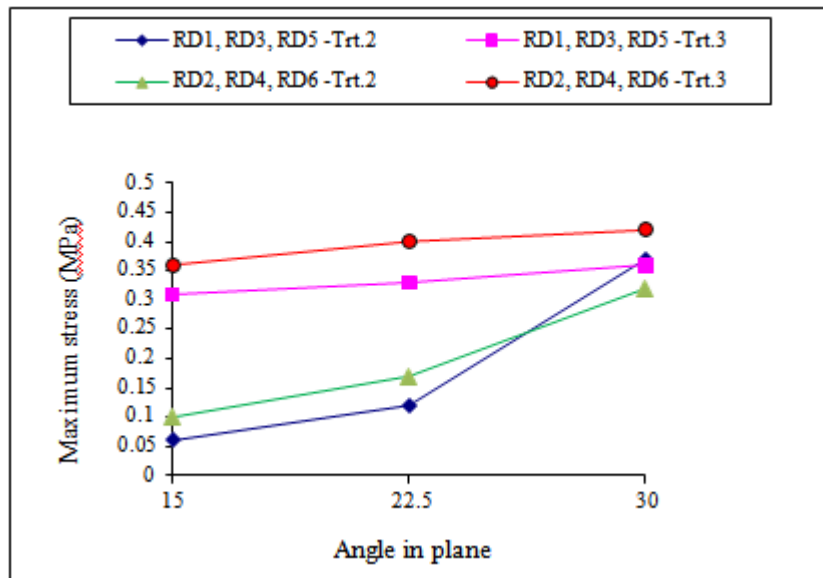


Figure (5) Maximum hoop tensile stress in brick

The meridional compressive stresses in brick for all models are shown in Fig (6). All Models analysed by Trt-2 method give compressive stresses much smaller than what Trt-3 method gives.

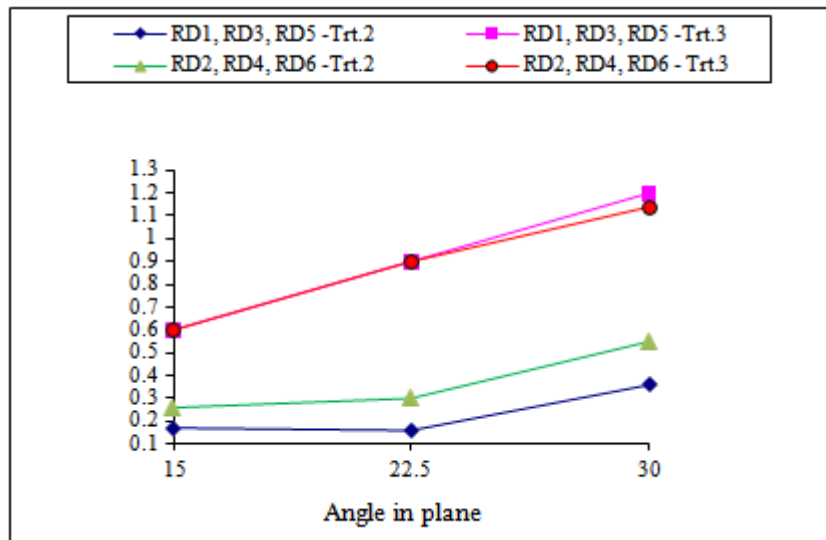


Figure (6) Maximum meridional compression stress in brick

In general, no tensile stresses in meridional direction of brick dome without ribs appear. In ribbed dome, tensile meridional stresses are observed in some cases as shown in Fig (7). In case of Trt-3 analysis, no tensile meridional stresses are found; this may be attributed to shell behaviour of such dome. Models (RD3, RD4, RD5 and RD6) with Trt-2 analysis exhibits tensile meridional stresses with values less than the permissible tensile stress of brick (0.2 MPa). However, models RD1 and RD2 do not reveal any meridional tensile stresses.

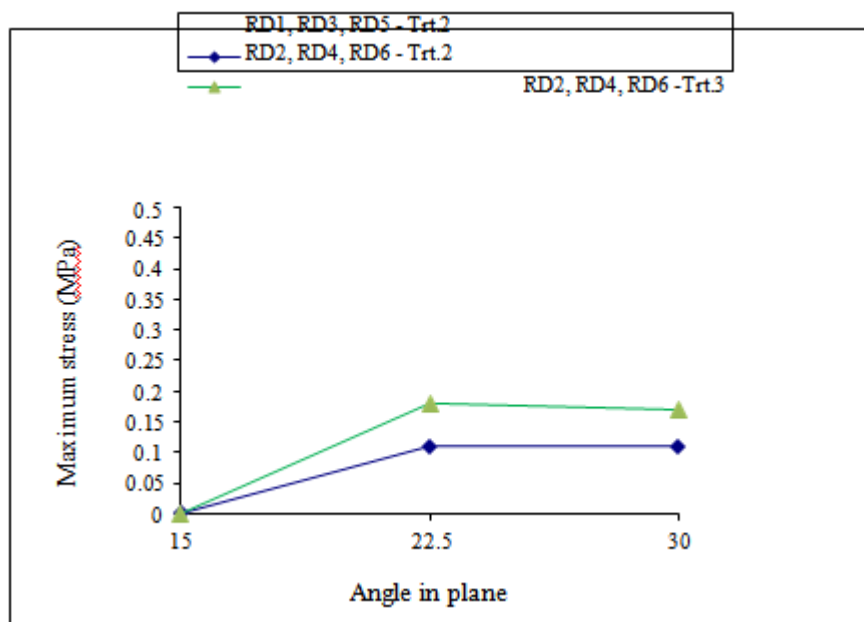


Figure (7) Maximum meridional tensile stress in brick

Table (3) shows the values of maximum hoop and meridional stresses of domes under the load combination. Figures (8), (9) and (10) show the hoop and meridional stress distribution for the brick dome and some of ribbed domes. Inspection of the Figures (9) and (10) reveals that the maximum value of tensile hoop stress is obtained near the base of dome at angle of embrace $\alpha = 90$ degrees. The results of the analysis show that brick dome of constant brick thickness 240 mm could not resist the applied loads because of the hoop tensile stress near bottom region (springing region) is greater than brick allowable tensile stress, while the compressive stresses are less than the allowable compressive stress of brick 0.8 MPa.

Table (3) Comparing of maximum stresses in different cases of domes

| Dome designation | Analysis method | Max. tension hoop stress (MPa) | Max. compression hoop stress (MPa) | Max. compression meridional stress (MPa) | Max. tension meridional stress (MPa) |
|------------------|-----------------|--------------------------------|------------------------------------|--|--------------------------------------|
| Brick dome BD | - | 0.60 | -0.34 | -0.60 | - |
| RD1 | Trt.2 | 0.06 | -0.04 | -0.18 | - |
| | Trt.3 | 0.34 | -0.14 | -0.60 | - |
| RD2 | Trt.2 | 0.11 | -0.06 | -0.27 | - |
| | Trt.3 | 0.38 | -0.15 | -0.60 | - |
| RD3 | Trt.2 | 0.12 | -0.12 | -0.16 | 0.11 |
| | Trt.3 | 0.35 | -0.11 | -0.9 | - |
| RD4 | Trt.2 | 0.19 | -0.13 | -0.32 | 0.20 |
| | Trt.3 | 0.18 | -0.08 | -0.30 | 0.20 |
| RD5 | Trt.2 | 0.40 | -0.40 | -0.37 | 0.14 |
| | Trt.3 | 0.38 | -0.14 | -1.18 | - |
| RD6 | Trt.2 | 0.35 | -0.18 | -0.6 | 0.20 |
| | Trt.3 | 0.45 | -0.15 | -1.2 | - |

Furthermore Figures (9) and (10) show the similarity in the stress distribution of the brick dome BD and the dome analysed by Trt-3 method. This confirms the previous conclusion that the ribs and rings lose their effect in analysis Trt-3.

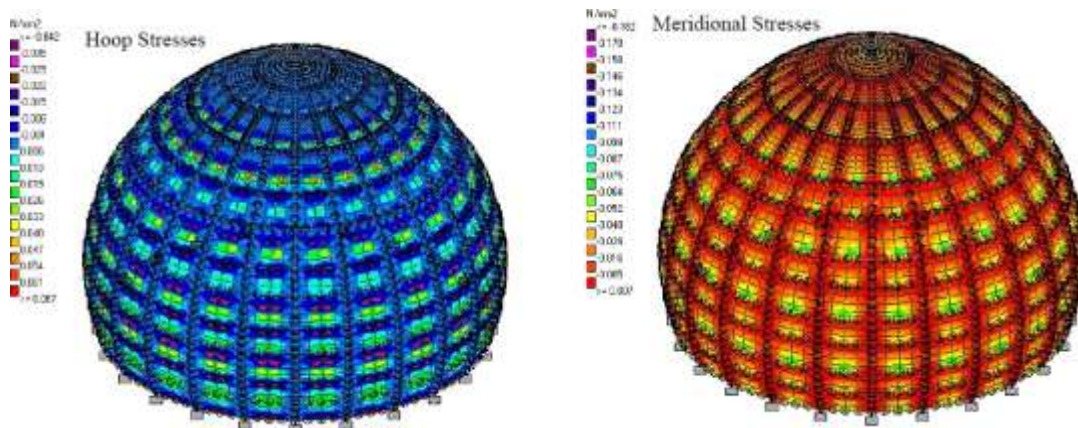


Figure (8) Stress distribution of RD1-Trt.2

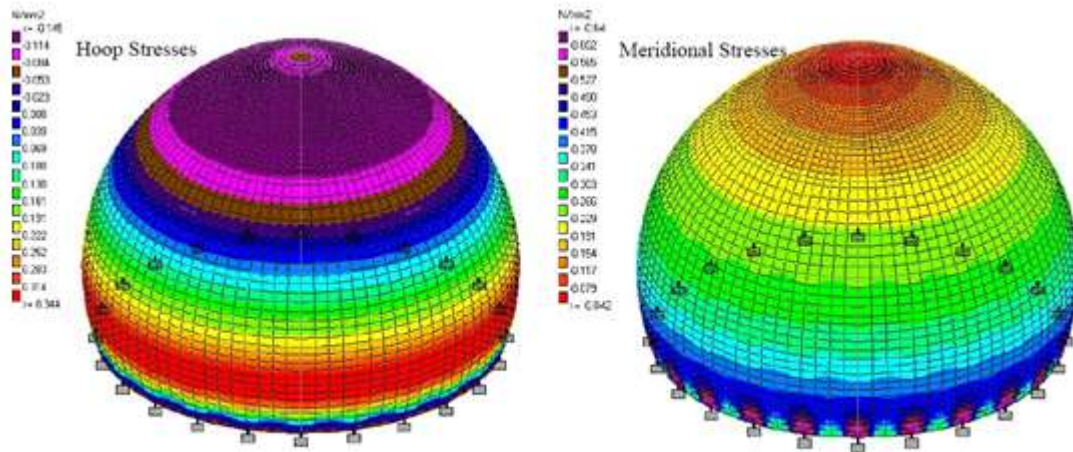


Figure (9) Stress distribution of RD1-Trt.3

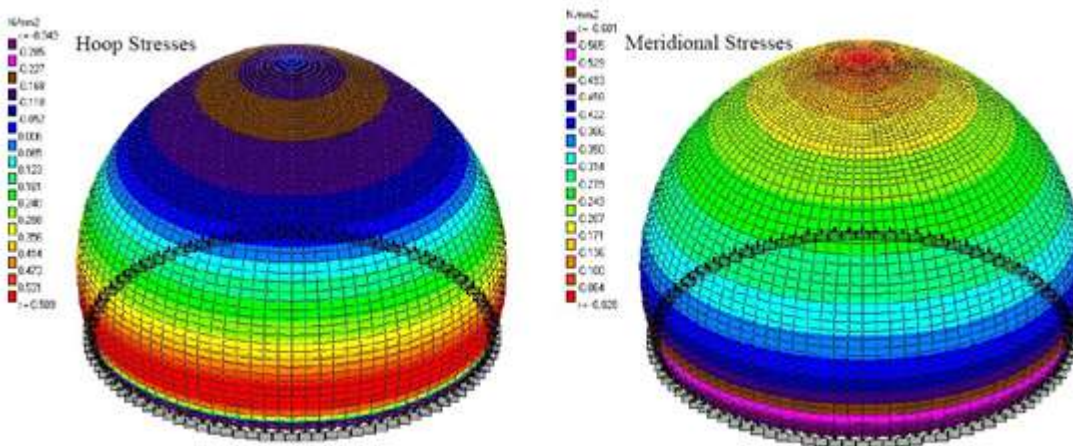


Figure (10) Stress distribution of BD

1.2 Deflection

In the three types of analysis, Trt-1, Trt-2 and Trt-3, the horizontal (ΔX) and vertical (ΔY) deflections are calculated. These deflections are determined for the ribbed domes in addition to the one without ribs, brick dome BD. Figures (11) and (12) show a sample of deflection shapes, and also Table (4) give the values of ΔX and ΔY for all analysed models.

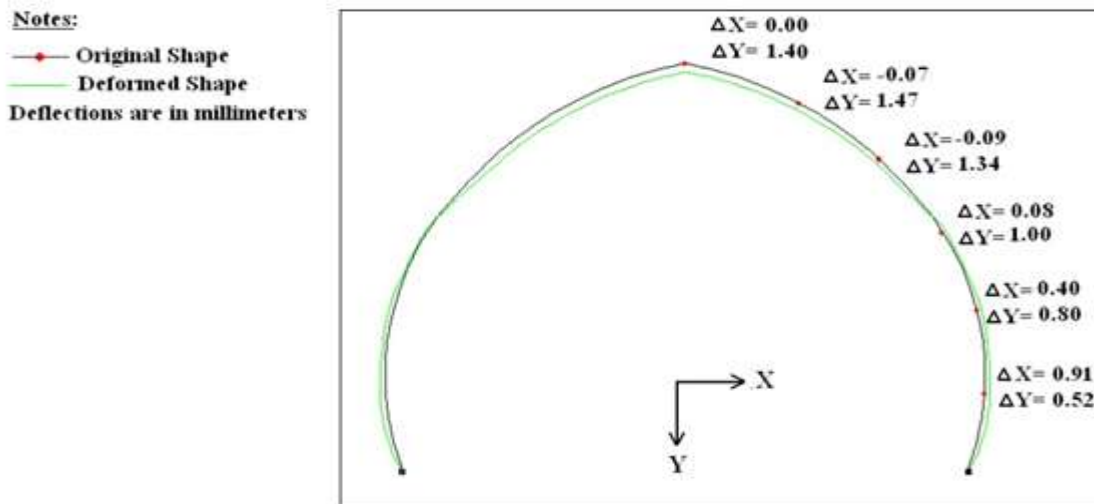


Figure (11) Deflection Shape of BD

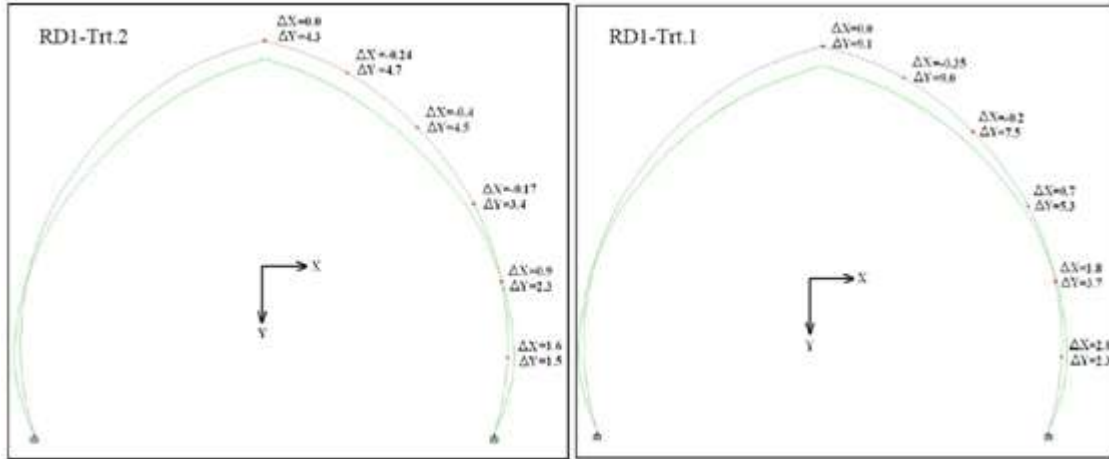


Figure (12) Deflection Shape of RD1

Table (4) Horizontal deflections ΔX

| Model Analysis Angle ϕ | Deflection ΔX (mm) | | | | | | | | | | | | |
|-----------------------------------|----------------------------|-------|-------|-------|-------|-------|-------|-------|-------|-------|-------|-------|-------|
| | BD | RD1 | | RD2 | | RD3 | | RD4 | | RD5 | | RD6 | |
| | General F.E.M. | Trt-1 | Trt-2 | Trt-1 | Trt-2 | Trt-1 | Trt-2 | Trt-1 | Trt-2 | Trt-1 | Trt-2 | Trt-1 | Trt-2 |
| 0° | 0.00 | 0.00 | 0.00 | 0.00 | 0.00 | 0.00 | 0.00 | 0.00 | 0.00 | 0.00 | 0.00 | 0.00 | 0.00 |
| 18° | -0.07 | -0.35 | -0.47 | -0.67 | -0.47 | -0.43 | -0.26 | -0.70 | -0.55 | -0.60 | -0.30 | -1.20 | -0.50 |
| 36° | -0.09 | -0.25 | -0.88 | -0.66 | -1.00 | -0.60 | -0.42 | -0.80 | -0.90 | -1.50 | -0.40 | -3.30 | -1.10 |
| 54° | 0.08 | 0.35 | 0.00 | 1.00 | 0.00 | 0.00 | 0.00 | 0.20 | 0.00 | -1.60 | 0.45 | -2.80 | 0.80 |
| 72° | 0.40 | 1.60 | 1.57 | 3.50 | 1.70 | 1.45 | 0.90 | 3.40 | 1.80 | 1.90 | 1.90 | 4.40 | 3.60 |
| 90° | 0.91 | 2.70 | 2.95 | 5.40 | 2.90 | 3.30 | 1.80 | 6.10 | 3.20 | 5.80 | 3.00 | 10.90 | 5.50 |
| 108° | 0.00 | 0.00 | 0.00 | 0.00 | 0.00 | 0.00 | 0.00 | 0.00 | 0.00 | 0.00 | 0.00 | 0.00 | 0.00 |

As it is shown in the Table and Figures the deflection is inwards (the negative values) for portions of dome and outward for other portions. Table (5) illustrate the values of angle ϕ (the angle of the point measured from the axis passing through the crown) at which the deflection equals to zero. The deflection ΔX for ϕ smaller than this value is negative and it is positive for value of ϕ larger than this value.

Table (5) Values of angle ϕ giving zero ΔX

| Analysis | Angle ϕ (degrees) | | |
|----------|------------------------|-------|----------------|
| | Trt-1 | Trt-2 | General F.E.M. |
| RD1 | 45 | 54 | - |
| RD2 | 45 | 54 | - |
| RD3 | 54 | 54 | - |
| RD4 | 52 | 54 | - |
| RD5 | 65 | 50 | - |
| RD6 | 65 | 50 | - |
| BD | - | - | 52 |

The maximum deflection ΔX is always obtained at α approximately equal to 90° . The brick dome BD shows smaller deflection ΔX than ribbed domes. The deflection ΔX of ribbed domes increases when the plan angle α increases or the ring spacing increases.

The method of analysis (Trt-1, Trt-2 and Trt-3) appears to have considerable effect on calculated deflection ΔX . Trt-1 method gives larger value of ΔX than Trt-2 method. These results are illustrated in Figs. (13) to (15). Except for model No. RD1, Trt-1 method gives a value of ΔX at $\alpha = 90^\circ$ which is double that of Trt-2 method.

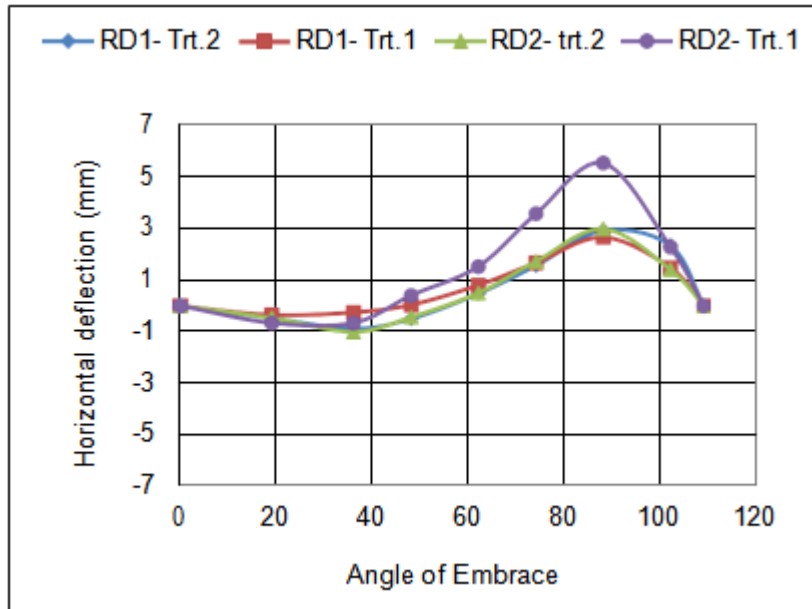


Figure (13) Horizontal Deflection Plan Angle 15°

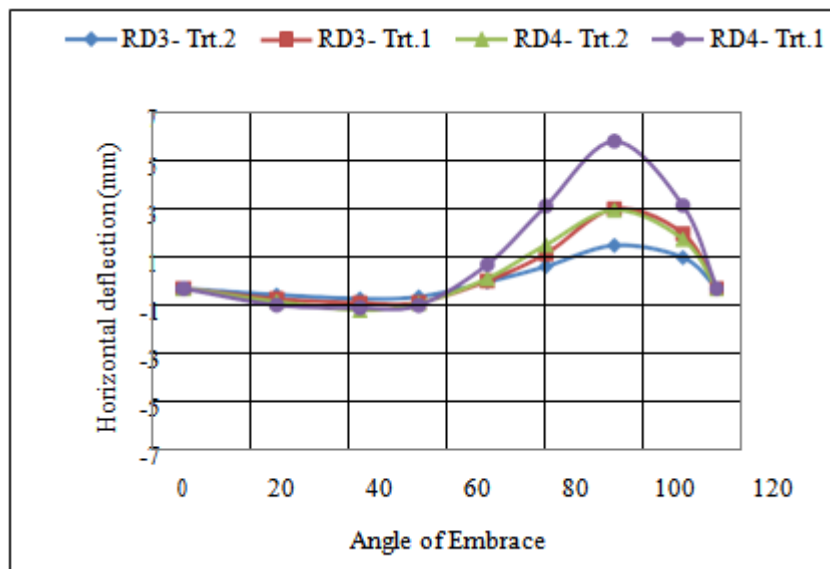


Figure (14) Horizontal Deflection - Plan Angle 22.5°

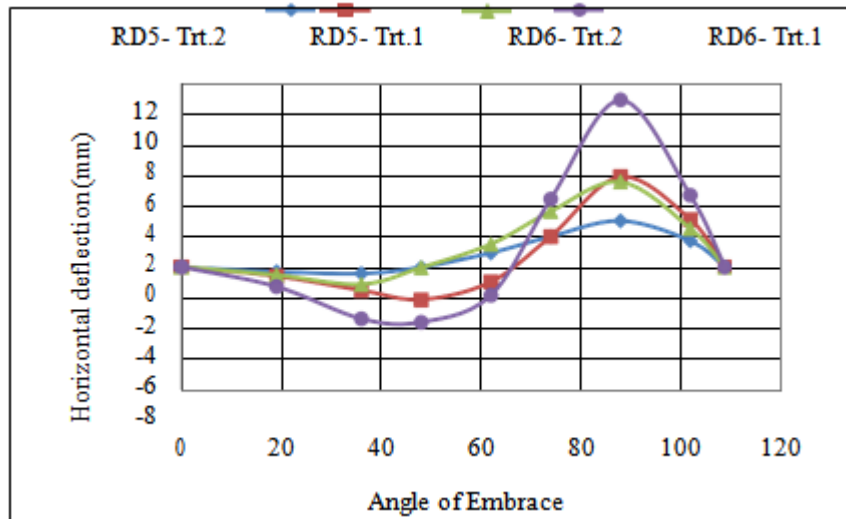


Figure (15) Horizontal Deflection - Plan Angle

Also shown in Figs. (11) and (12) the sample of horizontal and vertical deflection of some points on domes specified by the angle ϕ . Table (6) shows the values of ΔY for all models.

Table (6) Vertical deflections ΔY

| Model Analysis Angle ϕ | Deflection ΔY (mm) | | | | | | | | | | | | |
|-----------------------------------|----------------------------|-------|-------|-------|-------|-------|-------|-------|-------|-------|-------|-------|-------|
| | BD | RD1 | | RD2 | | RD3 | | RD4 | | RD5 | | RD6 | |
| | General F.E.M. | Trt-1 | Trt-2 | Trt-1 | Trt-2 | Trt-1 | Trt-2 | Trt-1 | Trt-2 | Trt-1 | Trt-2 | Trt-1 | Trt-2 |
| 0° | 1.40 | 9.06 | 8.90 | 9.90 | 4.00 | 11.41 | 6.36 | 11.67 | 6.10 | 12.86 | 9.20 | 12.00 | 9.00 |
| 18° | 1.47 | 9.00 | 9.78 | 10.74 | 5.10 | 11.48 | 6.76 | 12.32 | 7.20 | 13.32 | 9.50 | 14.40 | 10.10 |
| 36° | 1.34 | 7.75 | 9.64 | 9.70 | 5.60 | 10.46 | 6.47 | 11.34 | 7.22 | 13.25 | 9.00 | 16.00 | 10.50 |
| 54° | 1.00 | 5.85 | 7.65 | 6.90 | 4.10 | 8.40 | 5.25 | 9.10 | 5.76 | 11.50 | 7.00 | 13.90 | 7.70 |
| 72° | 0.80 | 3.90 | 5.30 | 4.37 | 2.65 | 5.80 | 3.64 | 5.80 | 3.78 | 7.70 | 4.80 | 8.60 | 5.00 |
| 90° | 0.52 | 2.70 | 3.70 | 3.00 | 1.80 | 3.90 | 2.50 | 4.00 | 2.60 | 5.24 | 3.40 | 5.70 | 3.50 |
| 108° | 0.00 | 0.00 | 0.00 | 0.00 | 0.00 | 0.00 | 0.00 | 0.00 | 0.00 | 0.00 | 0.00 | 0.00 | 0.00 |

The maximum value of deflection ΔY in brick dome occurs at the angle $\phi = 18^\circ$, however in ribbed dome models it is not the case. The maximum ΔY in ribbed domes occurs approximately between $\phi = 18^\circ$ and $\phi = 36^\circ$ as Table (6) shows and Figs. (16) to (18) illustrated. Also the same findings obtained for ΔX is noted for ΔY . These are represented in that the methods of analysis (Trt-1 and Trt-2) give different values of ΔY ; larger values are calculated by Trt-1 method, and increasing the plan angle ϕ and ring spacing lead to increase the ΔY , as can be seen in Table (6). Brick dome BD also gives smaller value of ΔY than ribbed domes.

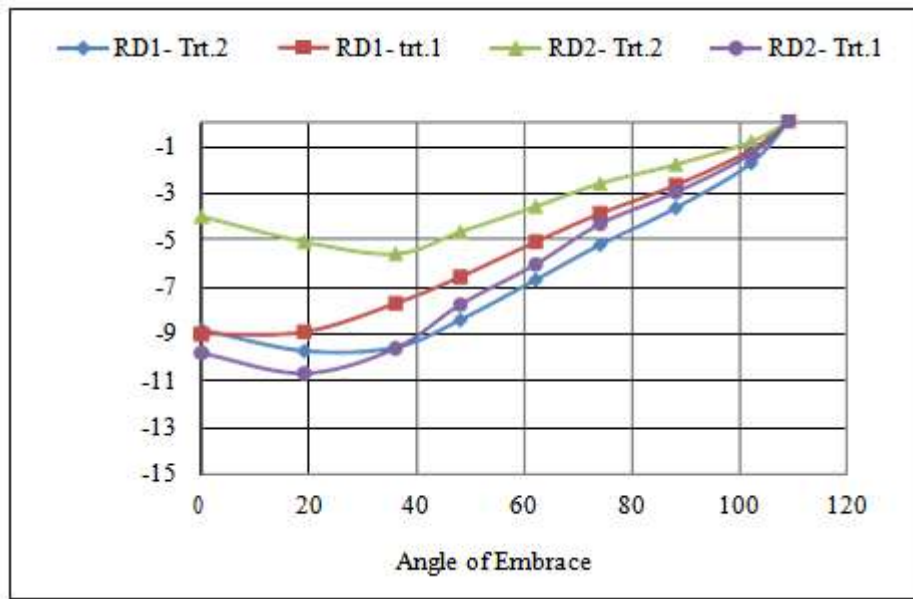


Figure (16) Vertical Deflection - Plan Angle 15°

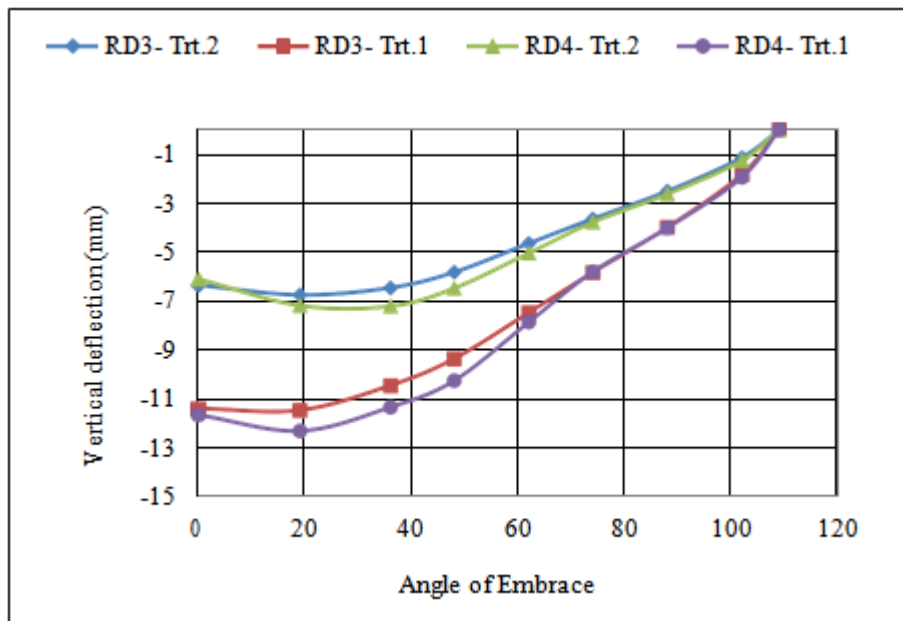


Figure (17) Vertical Deflection - Plan Angle 22.5°

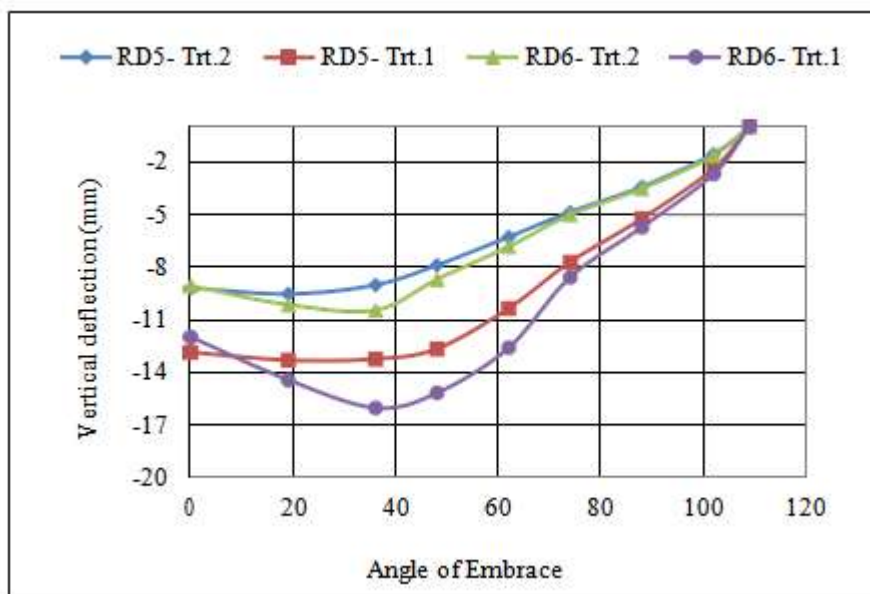


Figure (18) Vertical Deflection - Plan Angle 30°

VI. Conclusions

An analysis is conducted on brick domes with and without steel ribs and rings by using STAAD Pro. Software. The interaction between the bricks and steel ribs and rings is treated in different methods. In these methods the release facility given by the used software is utilized. It is found that the method of treatment has a considerable effect on stresses and deflections of domes.

The maximum horizontal displacement always occurs at a point having angle α equal to 90°. The vertical displacement occurs at the crown in the brick dome without steel ribs and rings, however, it is obtained at angle α between 18° and 36° in ribbed domes.

The hoop tensile and compressive stresses of brick decrease when the plan angle α of ribs decreases. However, when Trt-3 method of analysis is used the effect of α becomes ineffectual. It seems that the ribbed domes behave like ones without ribs in this method of analysis.

Tensile meridional stresses are found in brick of ribbed domes with plan angle $\alpha = 22.5^\circ$ and 30° when Trt-2 method of analysis is used. These stresses are less than the allowable tensile stresses. However, no tensile meridional stresses appear when $\alpha = 15^\circ$ and Trt-2 method are used or when Trt-3 method is used for all values of α .

References

- [1]. Chen, Wai-Fah and Lui, Eric M., " Hand Book of Structural Engineering", Taylor and Francis Group,2005.
- [2]. Heyman, J., "The Stone skeleton. 1st ed". New York: Cambridge University Press.1995.
- [3]. Chacko, Peter, Dipu, V. S. and Manju, P. M., "Finite element Analysis of Ribbed Dome", Trends and Recent Advances in Civil Engineering (TRACE- 24th -25th January 2014), International Journal of Engineering Research and Applications, 2014,25-32.
- [4]. Kaveha, A. and Talatahari, S., "Optimal design of schwelder and Ribbed Domes via a Hybrid Big Bang Big church Algorithm", Journal of Constructional Steel Research, Vol. 66, 2010, pp412-419.
- [5]. Al-Zaidi Emad Abed Abood, " Analysis of Reinforced Concrete Ribbed Domes Resting on Ring Beams and Columns", M.Sc. Thesis, Department of Building and Construction, University of Technology, Baghdad, Iraq,2013.
- [6]. Lau, Wanda W., " Equilibrium Analysis of Masonry Domes", M.Sc. Thesis, Massachusetts Institute of Technology,2006.
- [7]. International Conference of Building Officials and California Building Standards Commission, " Uniform Building Code- Vol. 2, USA,1997.